

Magnetic Coulomb Fields of Monopoles in Spin Ice and Their Signatures in the Internal Field Distribution

G. Sala¹, C. Castelnovo¹, R. Moessner^{2,*}, S. L. Sondhi³, K. Kitagawa⁴, M. Takigawa⁴, R. Higashinaka^{5,6}, and Y. Maeno⁵

¹ SEPnet and Hubbard Theory Consortium, Department of Physics,

Royal Holloway University of London, Egham TW20 0EX, United Kingdom

² Max-Planck-Institut für Physik komplexer Systeme, Dresden, 01187, Germany

³ Department of Physics, Princeton University, Princeton, NJ 08544, USA

⁴ Institute for Solid State Physics, University of Tokyo 5-1-5 Kashiwanoha, Kashiwa, Chiba 277-8581, Japan

⁵ Department of Physics, Graduate School of Science, Kyoto University, Kyoto 606-8502, Japan and

⁶ present address: Graduate School of Science, Tokyo Metropolitan University, Hachioji, Tokyo 192-0397, Japan

(Dated: July 26, 2012)

Fractionalisation – the breaking up of an apparently indivisible microscopic degree of freedom – is one of the most counterintuitive phenomena in many-body physics. Here we study its most fundamental manifestation in spin ice, the only known fractionalised magnetic compound in 3D: we directly visualise the $1/r^2$ magnetic Coulomb field of monopoles which emerge as the atomic magnetic dipoles fractionalise. We analyse the internal magnetic field distribution, relevant for local experimental probes. In particular, we present new zero-field NMR measurements which exhibit excellent agreement with the calculated lineshapes, noting that this experimental technique can in principle measure directly the monopole density in spin ice. The distribution of field strengths is captured by a simple analytical form which exhibits a low density of low-field sites—in apparent disagreement with reported μ SR results. Counterintuitively, the density of low-field locations decreases as the local ferromagnetic correlations imposed by the ice rules weaken.

Introduction — The magnetic field set up by a spin configuration is the most direct manifestation of the underlying magnetic moments. The discovery of a new spin state thus holds the promise of generating – and revealing its existence in – novel properties of the field it sets up.

A case in point is spin ice [1], which – uniquely among magnetic materials in three dimensions – exhibits an emergent gauge field and magnetic monopole excitations [2], which have analogies in magnetic nanoarrays [3–6]. The spin ice state has the great advantage of exhibiting phenomena of fundamental conceptual importance in a setting which as we describe below is simple enough to be easily and intuitively visualised: an order of topological nature manifests itself in the fractionalisation of the microscopic *dipole* degrees of freedom, leading to the deconfined magnetic *monopoles* [7].

Neutron scattering experiments, which provide magnetic field correlations in reciprocal space, have produced some of the strongest evidence so far for the gauge structure [8, 9] and ‘Dirac strings’ [10] that emerge at low temperatures. Another probe which has prominently been employed is muon spin rotation [11–13] (μ SR), which like NMR is sensitive to the local fields in real space. For such local probes, studies of the level of detail characteristic of the neutron analysis are still lacking.

We remedy this situation by computing the spatially resolved distribution of internal fields in spin ice. Most fundamentally, according to Ref. 2, the internal fields in spin ice contain a contribution from the underlying magnetic monopoles. Isolating and identifying this contribution is thus of great conceptual importance in corroborating the peculiar nature of these unique elementary excitations.

Here we show how to visualise the monopole contribution: by measuring the field strength at the considerably-sized magnetic voids of the lattice we find a radially symmetric signal (Fig. 4) which is well-described by the Coulomb law, $\propto 1/r^2$,

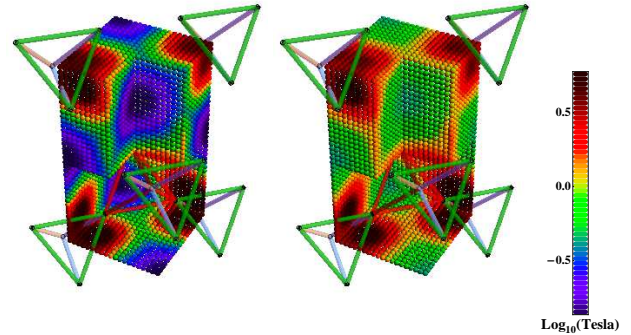


FIG. 1. Cross sections of the primitive unit cell. Left: Average field strength in 2in-2out spin ice configurations. The logarithmic colour scale ranges from dark blue (0.137 Tesla, the smallest average field strength recorded) to deep red (6 Tesla). Right: Average field strength in completely disordered Ising spin configurations.

with a coefficient that is in good agreement with the theoretical prediction [2]. Even if measuring the field strength deep inside the sample may be beyond the reach of current experiments, the Coulomb field of a magnetic monopole near the sample surface could be accessible to a sufficiently spatially resolved measurement.

To make contact with μ SR and NMR experiments, we compute the full field distribution in the unit cell (Fig. 1). This provides detailed predictions for NMR experiments, with the lineshape (Fig. 2) in excellent agreement with the first zero-field NMR measurements, the results of which we report here.

Our analysis places strong constraints on the μ SR signatures of the spin ice state. In particular, it seems highly unlikely that the signal detected in Ref. 12 is due to muons im-

planted in pristine bulk spin ice. (Our results are consistent with earlier estimates of the internal field strength at the muon site [11, 13, 14].)

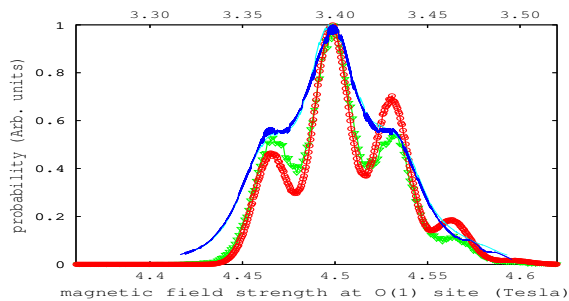


FIG. 2. Histograms of the magnetic field strength at the O(1) sites obtained from: experimental NMR data nominally at $T = 0.1$ K (blue) and at $T = 0.4$ K (cyan) – top axis; Monte Carlo simulations in equilibrium at $T = 0.6$ K (green) and equally weighted ensemble of 2in-2out spin ice configurations (red) – bottom axis. The experimental curves have been shifted so as to match the main peak position from numerics (see the Methods Section in the Supplemental Information); the vertical axis is chosen to set the maxima equal to unity.

In finer detail, we find that the internal field distribution fits well to a simple functional form at *all* temperatures (Fig. 3). Counterintuitively, we find an *enhancement* of the weak field

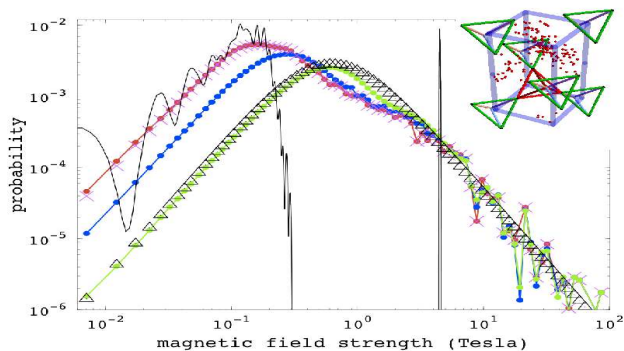


FIG. 3. Histograms of the field strengths across a uniform cubic grid spanning the primitive unit cell in a system of size $L = 4$ containing $16L^3 = 1024$ spins. Red: without monopoles. Magenta and blue: with two monopoles (see text). Green: random spin ice configuration (i.e., T much larger than any interaction energy scale). Black lines: centres of the super tetrahedra and of the rare earth tetrahedra (low and high field curves, respectively). Black triangles: $P(h) \sim h^2/(h^2 + H_0^2)^2$ fit to the random spin ice behaviour. Inset: Spatial distribution of locations of field strength smaller than 10 mTesla in *at least* one of the 10,000 statistically independent configurations sampled. The dimensionless volume fraction of such sites is approximately $5 \cdot 10^{-5}$.

sites as the temperature is lowered. This is surprising as spin ice is a ferromagnet – as defined by the sign of its Weiss temperature – and one might expect enhanced internal fields to appear as spins align. We interpret this unusual behaviour as a result of the interplay of the nanoscopic lattice structure of

spin ice and the slow decay of monopolar fields.

Overall, our analysis plugs two gaps: firstly, the conceptual one between the effective long-wavelength emergent gauge theory [2] and the nanoscale physics of the lattice; and secondly, the practical one between theory and real-space experimental probes.

Distribution of internal field strengths — In spin ice, the magnetic dipoles reside on the sites of the pyrochlore lattice, which consists of corner-sharing tetrahedra. We provide details of this structure as Supplemental Information but all that is necessary for digesting the following is: (i) in any of the exponentially numerous spin ice configurations, two spins point into each tetrahedron and two point out; and (ii) an (anti-)monopole corresponds to a tetrahedron with three spins pointing in (out).

In Fig. 3, we show histograms of the internal field distribution $P(h)$ collected across the primitive unit cell for three different classes of spin configurations (see the Methods Section in the Supplemental Information). We consider the cases of monopole-free states (red line) and of configurations containing two maximally separated monopoles, evaluating the field in a primitive cell containing a monopole (blue dots) or half way between the pair (magenta crosses). This is compared to a random configuration of Ising spins with local [111] easy axes, corresponding to an infinite temperature state (green).

In all cases, at small fields, $P(h) \propto h^2$, while at large fields, $P(h) \propto h^{-2}$. The latter reflects the geometric probability of probing the $1/r^3$ divergence of h close to a spin. The former is a non-trivial result which will play an important role in the interpretation of μ SR experiments further below; it implies that a site with a vanishing field is not ‘special’ in the sense that even an entirely flat probability distribution for each of the three components of the field vector would yield this functional form for $P(h)$.

The presence of a monopole is only weakly visible far away from it but nearby its effect is felt strongly – statistical weight is shifted from low to higher fields, whereas the overall shape of the distribution does not vary appreciably. This is highly counterintuitive, if one considers that spin ice 2in-2out tetrahedra are *ferromagnetically ordered*: all the spins point in the same direction, to the extent allowed by the local easy axes. For a ferromagnet, one would naively expect that the internal fields are larger in the 2in-2out arrangement than they are in presence of a monopole or otherwise disordered spins.

There are two reasons why this happens nonetheless. Firstly, the characteristic dipolar correlations between 2in-2out tetrahedra lead to an unusually large cancellation between fields from different tetrahedra. The spins form ‘flux loops’ where the sum of their dipole moments in fact vanishes. These ‘flux loops’ get broken down as monopoles appear, whose field decreases with distance *more slowly* than that of any dipole. This effect is captured by the dumbbell model [2], which accounts well for the long-wavelength aspect of the field distribution. [A more detailed explanation can be found in a dedicated section in the Supplemental Information for this paper.]

However, to reveal the second reason, such a picture needs to be supplemented to account for the detailed structure of the field distribution on the lattice scale. This exhibits considerable local structure, as shown in Fig. 1: near the spins, and at the centres of tetrahedra, there are large fields in excess of 4 Tesla. By contrast, in the voids between the spins, the fields average much lower. Most saliently, at the centres of supertetrahedra (see Fig. 4, inset), the probability of finding a low-field site is greatly enhanced (black dots, Fig. 3). Indeed, the oscillations in this latter curve provide a crucial pointer: at these locations, aided by symmetry, the fields of nearby spins can cancel locally, leaving a lower characteristic field scale, and hence enhanced low-field probability.

This shows up in the field distribution averaged across a unit cell near a monopole (Fig. 3, magenta line), which follows the form $P(h) \sim h^2 / (h^2 + H_0^2)^2$ derived for the distribution of fields due to randomly located and oriented spins [15]. Crucially, the value of H_0 is *reduced* compared to that of a defect-free configuration (red line). This picture is backed up by the good fit of the above equation to a high-temperature state corresponding to a collection of randomly oriented [111]-easy-axis dipoles (green line), and hence a high density of randomly distributed monopoles.

Finally, Fig. 1 directly demonstrates that, along with the breaking of ice rules, the spontaneous spatial organisation of fields strengths into high- and low-field locations within the unit cell is suppressed.

Average field due to magnetic monopoles — Having analysed the spatial distribution of fields inside the unit cell, we next turn to visualising the field set up by a monopole. Recall that magnetic monopoles experience a relative force of Coulombic nature. We ask: can one also measure the corresponding magnetic field $(\mu_0/4\pi)(q/r^2)$? This is difficult for two reasons. Firstly, the internal field away from the lattice sites varies tremendously between configurations. Secondly, the ‘Dirac string’ [2] emanating from the monopole carries a magnetisation, \vec{M} , which cancels off the field, \vec{H} , to give a net $\vec{\nabla} \cdot \vec{B} = \mu_0(\vec{\nabla} \cdot \vec{H} + \vec{\nabla} \cdot \vec{M}) = 0$. These two issues can be taken care of by (i) averaging over many configurations (or, in experiment, over time whilst keeping the observed monopole position fixed) and (ii) measuring the field at points as far away as possible from any lattice sites. (This also minimises the strong near-field of the spins.)

In Fig. 4, we display the direction of the average fields at the centres of the supertetrahedra set up by two stationary monopoles, which visually reproduce the expected hedgehog-like monopolar field pattern. We have verified that by subtracting the analytical Ewald-summed field for two point monopoles with charge given in Ref. 2, the residual fields appear randomly oriented with average strength tenfold suppressed.

To be more quantitative, in Fig. 4 we show the average field (over 10^6 configurations) evaluated along a line joining the two monopoles halfway across a system of 128,000 spins ($L = 20$), along the [001] direction. The Coulomb field predictions are borne out, but masked in part by the line passing

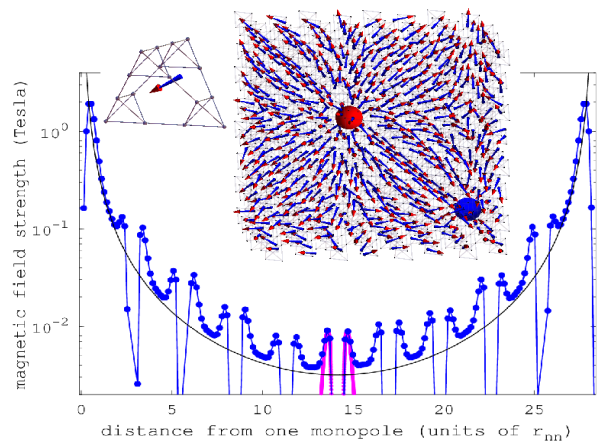


FIG. 4. Top: Illustration of the magnetic field due to the monopoles (red and blue spheres) at the centres of the super-tetrahedra of the pyrochlore lattice, visualised by unit vectors in the local field direction (red-blue arrows), for 1024 spins with periodic b.c., averaged over 10,000 independent configurations. As shown, each super-tetrahedron is formed by 4 regular tetrahedra in the lattice. The super-tetrahedra centres are (locally) the farthest points from any spin on a pyrochlore lattice site. Bottom: Averaged fields along the [001] line joining two monopoles (connected blue dots). The leading behaviour is captured, to within 20% error, by the Ewald-summed field from two point magnetic charges at the locations of the monopoles, with charge from the theoretical prediction [2], $2\mu/a_d \simeq 4.6 \mu_B/\text{\AA}$ (black line). The periodic deviations from the Coulomb form are due to spins which sit very close to the line – this contribution is explicitly shown in magenta for the spin at the midpoint between the monopoles).

very close to spins, which contribute a strong and periodic deviation (magenta line) from the theoretical curve at positions $2\sqrt{2}n$, $n = 0, \dots, 10$ (in units of r_{nm}).

It is tempting to speculate that, if a quantum spin ice material were to be discovered where monopole motion can be made slower than quantum dynamics of spin-rearrangements preserving the ice rules, the internal fields would be due almost entirely to the emergent magnetic monopoles!

Experiment I: Zero-field NMR at the O(1) sites — Given the ferromagnetic interactions, the centres of the rare earth tetrahedra experience a large internal field of several Tesla (from numerical simulations using Ewald-summed interactions and fields – see the Methods Section in the Supplemental Information for further details), which as we show next can be used to distinguish between tetrahedra which host monopoles, and those which do not.

The centres of the rare earth tetrahedra in the pyrochlore lattice are occupied by oxygen ions (customarily referred to as O(1) oxygens). The ^{17}O isotopes are NMR active and can be used to detect the internal fields in a zero field NMR measurement. Indeed, two of the present co-authors have carried out the first NMR experiments on the ‘monopole-free’ line as shown in Fig. 2. Also shown is a comparison to Monte Carlo simulations in thermal equilibrium. The agreement of the line-

shape is remarkably good. The experimental spectrum is actually peaked at 3.4 Tesla, i.e., about 25% below the calculated peak. This shift is most likely due to spatial distribution of Dy-4f electrons causing deviations from a point dipole approximation (multipolar effects) and/or effects of Dy-O chemical bonding.

A promising aspect of these NMR measurements lies in the possibility of direct detection of monopoles. Indeed, when a tetrahedron hosts a monopole, the field at its O(1) site drops by approximately 13%. This effect is 3 times larger than the linewidth due to variations in the field at the O(1) site because of neighbouring monopoles or more distant spins. Therefore, the relative intensity of the NMR signal at this pair of field values provides a quantitative measure of the density of monopoles. In practice, small densities may be hard to detect above the background. Also, monopoles must not move over the time scale of NMR spin-echo experiments (a few tens of microseconds) to be detected as a distinct resonance line. Given the insights from modelling AC susceptibility results, which suggest a hopping rate in the range of milliseconds [16, 17], this condition seems comfortably achievable.

Experiment II: μ SR — The other major probe of the local magnetic fields is μ SR. Indeed, Ref. 12 has reported using μ SR experiments to measure the monopole charge via an ingenious analogy to the Wien effect familiar from electrolytes. This is currently a contested experiment [13] and we would like to make a few observations on it from the perspective of the current paper.

First, we note that one important feature of the data presented in Ref. 12 is that their signal was extracted from sites where the muons experience very low fields, of order a few milliTesla. This follows from the observation that doubling a transverse field of strength 1 mTesla doubles the μ SR precession frequency. From our work it is clear that there is a *very low density* of such sites (see Fig. 3), located preferentially near the centres of supertetrahedra (Fig. 1). It thus seems very unlikely that the substantial muon signal emanates from sites in the pristine bulk.

Second, the analysis of Ref. 12 invokes two distinct phenomena: first, the applied magnetic field induces an increase in the monopole density; and second, this increase leads to an enhanced depolarization rate. The first feature is indeed an expected phenomenon for the steady state of electrolytes in a field, but for spin ice, it can only occur as a transient: since monopole motion magnetises the sample, there can be no steady state with a nonzero monopole current. Moreover, in thermal equilibrium, the density of monopoles is believed to decrease in an applied field. About this our present work has nothing to say.

However regarding the second step, our results indicate that a field-induced regime with heightened monopole density would be accompanied by a depletion of low-field sites. At least this aspect is qualitatively in keeping with the finding in Ref. 12 that the rate of decay of the μ SR asymmetry gets larger in the Wien setting as the applied field is increased.

Third, combining the above observations leads us to con-

sider the interesting possibility that the signal arises from the action of an enhanced monopole density on muons implanted *outside* the sample. The idea here is that outside the sample the monopole fields would dominate over the much smaller fields present in their absence—given that the field of a monopole decays less slowly than that of an isolated spin. [Interestingly, it was very recently suggested in Ref. 13 that the signal from muons inside the sample is lost altogether because of large (compared to 1 mTesla) and fast magnetic fluctuations and that the only measurable signal due to spin ice comes from muons implanted outside, sensitive to stray fields, which are analysed in Ref. 18.]

A very rough estimate based on a monopole liquid subject to Debye screening [19] suggests that in the temperature range $T \sim 0.2 - 0.5$ K, the magnetic field set up by a monopole measured a distance roughly 100 ± 50 Å from the sample surface both lies in the range relevant for μ SR (between 0.1 and 1 mTesla) and dominates that set up by an individual spin in the sample. Note that – unlike stray fields set up by the magnetisation induced by a uniform external field – the monopole density grows with temperature, thus providing a qualitative discriminant between the two. A combined study of temperature-dependent (uniform) susceptibility and μ SR experiments therefore looks like the most prominent direction to make progress on this issue.

All such considerations point to the need for more detailed studies of what happens near the surface of a sample [20] – e.g., what happens to the surface monopole density (as a function of time and field)? Moreover, little is known at present concerning the surface of spin ice samples, e.g., what the nature of the local crystal fields is or how the magnetic lattice terminates. It is also worth bearing in mind that equilibration in spin ice may be incomplete at low temperatures, as the equilibrium monopole density vanishes exponentially – at 70 mK, the lowest temperature accessed so far in μ SR measurements, their number density is estimated to be such that there is only one pair for a *macroscopic* volume of a quarter of a cubic metre!

Finally, we would be remiss if we did not note that our considerations here have entirely to do with spatially fluctuating static fields and their dephasing of muon precession, whereas Ref. 13 proposes that large dynamical fluctuations are present. The tension between their proposal and the magnetic susceptibility data that are consistent with much slower dynamics for the spins will need to be resolved before a consistent account of spin dynamics in spin ice can be given.

Conclusions — We have provided a way of visualising the magnetic field of a magnetic monopole inside spin ice, yielding the first nanoscopic real space picture of this fractionalised excitation. Our work attests to the reality of the monopolar magnetic field not only at long wavelengths but also on the lattice scale.

As experimental proofs of the existence of monopoles move in the direction from thermodynamics towards increasingly microscopic ‘single-monopole’ detection, we hope that this work will lay the theoretical groundwork for future searches,

such as the ones using NMR or local field probes outside the sample which we have outlined above.

Acknowledgments — We thank Steves Blundell and Bramwell, Sarah Dunsiger, Sean Giblin, Chris Henley, Jorge Quintanilla, and Tomo Uemura for several useful discussions.

G.S. and C.C. are grateful to ISIS at the Rutherford Appleton Laboratories for hospitality and financial support. This work was supported in part by EPSRC Postdoctoral Research Fellowship EP/G049394/1 (C.C.). We mutually acknowledge hospitality and travel support for reciprocal visits.

-
- [1] S. T. Bramwell and M. J. P. Gingras, *Science* **294**, 1495 (2001).
 - [2] C. Castelnovo, R. Moessner, and S. L. Sondhi, *Nature* **451**, 42 (2008).
 - [3] R. F. Wang, et al., *Nature* **439**, 303 (2006).
 - [4] G. Möller and R. Moessner, *Phys. Rev. B* **80**, 140409(R) (2009).
 - [5] S. Ladak, D. E. Read, G. K. Perkins, L. F. Cohen, and W. R. Branford, *Nature Phys.* **6**, 359 (2010).
 - [6] E. Mengotti, et al., *Nature Phys.* **7**, 68 (2010).
 - [7] C. Castelnovo, R. Moessner, and S. L. Sondhi, *Annu. Rev. Condens. Matter Phys.* **3**, 35 (2011).
 - [8] T. Fennell, et al., Magnetic Coulomb phase in the spin ice $\text{Ho}_2\text{Ti}_2\text{O}_7$. *Science* **326**, 415-417 (2009).
 - [9] H. Kadowaki, et al., *J. Phys. Soc. Japan* **78**, 103706 (2009).
 - [10] D. J. P. Morris, et al., *Science* **326**, 411 (2009).
 - [11] J. Lago, S. J. Blundell, and C. Baines, *J. Phys.: Condens. Matter* **19**, 326210 (2007).
 - [12] S. T. Bramwell, et al., *Nature* **461**, 956 (2009).
 - [13] S. R. Dunsiger, et al., *Phys. Rev. Lett.* **107**, 207207 (2011).
 - [14] S. R. Dunsiger, et al., *Phys. Rev. B* **54**, 9019 (1996); S. R. Dunsiger, R. F. Kiefl, and J. S. Gardner, TRIUMF Annual Report (2000).
 - [15] N. Rivier and K. Adkins, in *Amorphous Magnetism*, edited by H. O. Hooper and A. M. de Graaf (Plenum, New York, 1973), p. 215.
 - [16] J. Snyder, et al., *Phys. Rev. B* **69**, 064414 (2004).
 - [17] L. D. C. Jaubert and P. C. W. Holdsworth, *Nature Phys.* **5**, 258 (2009).
 - [18] S. J. Blundell, *Phys. Rev. Lett.* **108**, 147601 (2012).
 - [19] C. Castelnovo, R. Moessner, S. L. Sondhi, *Phys. Rev. B* **84**, 144435 (2011).
 - [20] I. A. Ryzhkin and M. I. Ryzhkin, *JETP Lett.* **93**, 384 (2011).

SUPPLEMENTAL INFORMATION

Spin ice basics

Here, we briefly collate some basic facts about spin ice – the reader interested in a more detailed and complete overview is referred to Ref. 1 and the forthcoming Ref. 2.

The canonical spin ice materials are $\text{Dy}_2\text{Ti}_2\text{O}_7$ and $\text{Ho}_2\text{Ti}_2\text{O}_7$. The magnetic ions Dy^{3+} and Ho^{3+} live on a lattice of corner sharing tetrahedra (pyrochlore lattice) and they have large effective spins: $J = 15/2$ and $J = 8$, respectively. A strong local easy axis anisotropy forces the spins to lie along the lines connecting the centres of adjacent tetra-

hedra (namely, the local $[111]$ axis, see Fig. 5). The combi-

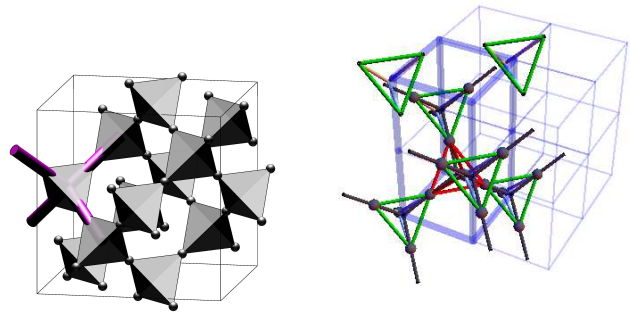


FIG. 5. Left panel: Illustration of the pyrochlore lattice. Right panel: Conventional cubic unit cell in spin ice, containing 16 spins (dark gray spheres). The side of the cell equals $2\sqrt{2}r_{\text{nn}}$, where r_{nn} is the pyrochlore lattice nearest-neighbour distance. A primitive unit cell (highlighted by thick blue lines) is 4 times smaller than the cubic unit cell and contains only 4 spins. The black lines are the bonds of the diamond lattice formed by the centres of the tetrahedra and they identify the local $[111]$ axes of the rare earth magnetic moments. The distance between the centres of two neighbouring tetrahedra is given by the diamond lattice constant, $a_d = \sqrt{3/2}r_{\text{nn}}$.

nation of large electronic spins and strong easy axes leads to large magnetic moments of the order of 10 Bohr magnetons per spin. The long range dipolar interactions are dominant. To a good approximation, the full Hamiltonian of these systems can be written as

$$H = J_{\text{ex}} \sum_{\langle i,j \rangle} \mathbf{S}_i \cdot \mathbf{S}_j + \frac{\mu_0 \mu^2}{4\pi} \sum_{i < j} \left[\frac{\mathbf{S}_i \cdot \mathbf{S}_j}{r_{ij}^3} - \frac{3(\mathbf{S}_i \cdot \mathbf{r}_{ij})(\mathbf{S}_j \cdot \mathbf{r}_{ij})}{r_{ij}^5} \right], \quad (1)$$

where the summation is over the indices i, j of the spins on the lattice, $J_{\text{ex}} > 0$ is the exchange coupling constant, μ_0 is the vacuum permeability, and $\mu \simeq 10\mu_B$ is the magnetic dipole moment of a spin.

The interplay between the strong local easy axes and the dipolar interactions favours nearest-neighbour ‘pseudospin antiferromagnetism’: a spin pointing into a given tetrahedron wishes its neighbors on the same tetrahedron to point out and vice versa. The resulting ground-state configuration are described by the ice rules, which stipulate that two spins point in and two point out of each tetrahedron. Exponentially many configurations satisfy the ice rules, leading to an *extensive* low-temperature entropy of $S_p \approx \frac{1}{2} \log \frac{3}{2}$, as verified experimentally by Ramirez *et al.* [4]. Hence, despite a ferromagnetic Curie-Weiss temperature $\approx 2K$, the spin ice compounds fail to develop long-range spin order down to a temperature four times lower.

This peculiar degeneracy has two remarkable consequences. Most basically, the spin correlators are characterised by an emergent gauge symmetry, which results from an effective conservation law for the magnetisation density which

is implied by the ice rules—the effective theory of spin ice is an emergent magnetostatics. In such a theory, the elementary excitations in spin ice do not take the conventional form of extended domain walls. Rather, flipping a spin in a 2in-2out state generates two defective tetrahedra which have 3in-1out and 3out-1in spins, respectively. These defects are then free to move through the system by means of spin flip processes that do not generate further defects: the initial dipolar perturbation (a spin flip) fractionalises into two point like excitations (the two defective tetrahedra). Indeed, one can formally show that these excitations are truly deconfined [3], being subjected only to a Coulombic ($1/r$) interaction potential.

These defects can be shown to carry a net magnetic charge, so that spin ice is the first experimentally accessible setting where free point-like magnetic charges can be observed and manipulated.

Flux loops and temperature dependence of the internal fields

In order to understand this counterintuitive temperature dependence of the distribution of low field sites in spin ice materials, it is useful to note that this system is very unusual in that it is a magnet in which *ferromagnetism* appears in a frustrated way.

(1) *Ferromagnetism*: at a single tetrahedron level, the dipolar interactions are minimised by a ferromagnetic arrangement of the spins. The well-known 2in-2out ice rules maximise indeed the magnetic moment of a tetrahedron. (2) *Frustration*: the degeneracy resulting from the frustration-induced underdetermination leads to longer range correlations, where the local moments do not align, like in a usual ferromagnet, and hence do not produce a macroscopic moment. Rather, the (effective) emergent gauge structure is one which suppresses the coarse-grained moments locally. [5] Pictorially and intuitively (if not rigorously), this can be understood by the dipoles aligning head-to-tail to form strings which have a preference for closing back on themselves. Such strings exhibit zero net mono- and dipole moments in a continuum treatment, which in turn leads to an effective suppression of the fields they produce at large distances.

When monopoles are present, the formation of the closed loops breaks down as monopoles introduce endpoints of such loops. [An open loop terminated by monopoles is commonly referred to as a 'Dirac string' in the literature.] Therefore, the rapid decay of the loop field due to the vanishing of the monopole and dipole moments is replaced by the slow decay of the Coulomb field.

The fields due to a distribution of monopoles thus combine to give an enhanced typical field strength, and hence a concomitant reduction in the density of low-field sites. This explains the observed effect.

Indeed, this behaviour is immediately apparent in the dumbbell model introduced in Ref. 3. In that model, each spin is replaced by a dumbbell of charges located at the opposite ends of the lattice vector separating the centres of two adjacent

tetrahedra. When the ice rules are satisfied throughout the system, two positive and two negative charges overlap at the centre of each tetrahedron. This leads to a charge neutral system that gives rise to vanishing internal fields. Adding monopoles replaces the effectively charge-neutral field-free system with one in which charges are distributed throughout, leading to a complex superposition of 'stray fields' of all the monopoles at any given site of the lattice.

These arguments neglect features of the short-distance behaviour, which as we show in this work are themselves non-trivial. In particular, lattice-scale variations of the field are substantial, ensuring the (energetically required) decrease of the effective field strength at the sites of the spins as monopoles are created with increasing temperature.

Now, low-field sites occur due to the cancellation of the strong fields of nearby spins. The probability of such local cancellation is not much influenced by the presence of a distant monopole; however, even if such local cancellation takes place, it is then spoiled by the above mentioned monopolar 'stray fields'. Hence, the occurrence of low-field sites is suppressed by the creation of monopoles.

Methods

Statistically independent spin configurations were obtained by means of loop updates that do not introduce violations to the 2in-2out ice rules and do not alter the location or charge of existing monopoles in the system. The internal fields for each configuration were obtained using the Ewald summation technique [6], with the $\text{Dy}_2\text{Ti}_2\text{O}_7$ parameters given in Ref. 7.

The average field strengths in Fig. 1 in the manuscript and the histograms in Fig. 3 in the manuscript were obtained from a uniform cubic grid of 16,000 points (corresponding to a point spacing of $< 0.25 \text{ \AA}$) across a primitive unit cell of the system (Fig. 5), averaged over $\sim 10^4$ realisations.

The Monte Carlo simulations that produced the distribution in Fig. 2 in the manuscript used single spin flip updates and Ewald-summed dipolar interactions between the spins, for a system of 3,456 spins ($L = 6$).

The O-NMR experiments requires ^{17}O , which is the only oxygen isotope with a non-zero nuclear magnetic moment. We have enriched ^{17}O content in a crystal of $\text{Dy}_2\text{Ti}_2\text{O}_7$ grown by a floating-zone image furnace from the natural abundance of 0.01% to approximately 50% by annealing the crystal under 65% $^{17}\text{O}_2$ gas at 1000°C for several days. Only the O(1) sites at the 8a positions located at the centers of the Dy-tetrahedra experience large internal fields $\gtrsim 3$ Tesla, while the internal fields at the O(2) sites at the 48f positions are much smaller and do not contribute to the observed signal. Moreover the electric field gradient is zero at the O(1) sites. Therefore, the NMR spectrum at the O(1) site represents the distribution of the local fields (directly obtained by dividing the frequency by 5.77185 Tesla/MHz, which is the gyromagnetic ratio of ^{17}O nuclei). To construct a broad-band spectrum, each Fourier spectrum of a pulsed NMR echo is summed

while the frequency is being swept (Fourier-step-summing technique). Low-temperature experiments have been carried out by putting the sample into a one-shot liquid ^3He fridge or into a dilution fridge using a He mixture.

Further experiments

Surface experiments

Ideally, we would like to measure the monopole field (Fig. 4 in the manuscript) by placing probes at the centres of supertetrahedra. Interestingly, these coincide with the centres of tetrahedra of titanium ions. Placing an NMR-active ion there would in principle allow access to the Coulombic form of the internal fields.

However, even if this remains a thought experiment for the time being, it is clear that a promising strategy is to suppress short-distance fluctuations by moving away from spin locations even on the scale of a lattice constant (Fig. 4 in the manuscript). The obvious way to do this is to probe the fields close to the surface of a sample, as discussed in the previous section. The spins and strings being confined to the sample, one can thus hope to see the farther-ranging monopole magnetic field undisturbed. Indeed, it is such a set-up that was proposed by Zhang *et al.* [8] to measure the image magnetic monopole induced by an electric charge near the surface of a strong topological insulator.

Magnetic avalanches

Our work also sheds light on a range of non-equilibrium phenomena recently measured in spin ice [10], and their prominent analogues in artificial spin ice [11, 12]. While the field strength throughout the unit cell fluctuates wildly, the

field projected onto the spin direction on a lattice site is known to be near constant for an ‘ideal’ interaction [S. V. Isakov, R. Moessner, and S. L. Sondhi [9]; for the conventional dipolar Hamiltonian, we find a broadening to 0.80 ± 0.03 Tesla. This field sets the energy scale for creating bound monopole pairs at low temperature. This quantity – as well as the Coulomb interaction between two monopoles as they separate – is important for triggering the avalanches which have received much attention of late [10–12].

-
- [1] S. T. Bramwell and M. J. P. Gingras, *Science* **294**, 1495 (2001).
 - [2] C. Castelnovo, R. Moessner, and S. L. Sondhi, *Annu. Rev. Condens. Matter Phys.* **3**, 35 (2011).
 - [3] C. Castelnovo, R. Moessner, and S. L. Sondhi, *Nature* **451**, 42 (2008).
 - [4] A. P. Ramirez, A. Hayashi, R. J. Cava, R. Siddarthan, and B. S. Shastry, *Nature* **399**, 333 (1999); for an interesting, much earlier, precursor see H. W. Blöte, R. F. Wierling, and W. J. Huiskamp, *Physica* **43**, 549 (1969).
 - [5] D. A. Huse, W. Krauth, R. Moessner, and S. L. Sondhi, *Phys. Rev. Lett.* **91**, 167004 (2003).
 - [6] S. W. de Leeuw, J. W. Perram, and E. R. Smith, *Proc. R. Soc. Lond. A* **373**, 27 (1980); S. W. de Leeuw, J. W. Perram, and E. R. Smith, *Proc. R. Soc. Lond. A* **373**, 57 (1980).
 - [7] B. C. den Hertog, and M. J. P. Gingras, *Phys. Rev. Lett.* **84**, 3430 (2000).
 - [8] X.-L. Qi, R. Li, J. Zang, and S.-C. Zhang, *Science* **323**, 1184 (2009).
 - [9] S. V. Isakov, R. Moessner, and S. L. Sondhi, *Phys. Rev. Lett.* **95**, 217201 (2005).
 - [10] D. Slobinsky, et al., *Phys. Rev. Lett.* **105**, 267205 (2010).
 - [11] P. Mellado, O. Petrova, Y. Shen, and O. Tchernyshyov, *Phys. Rev. Lett.* **105**, 187206 (2010).
 - [12] E. Mengotti, L. J. Heyderman, A. Fraile Rodríguez, F. Nolting, R. V. Hügli, and H.-B. Braun, *Nature Phys.* **7**, 68 (2010).